



Article

Thermal, X-ray Diffraction and Oedometric Analyses of Silt-Waste/NaOH-Activated Metakaolin Geopolymer Composite

Daniele Moro ^{1,*}, Riccardo Fabbri ¹, Jennifer Romano ¹, Gianfranco Ulian ¹, Antonino Calafato ¹, Abbas Solouki ^{2,3}, Cesare Sangiorgi ² and Giovanni Valdrè ^{1,*}

- ¹ Centro di Ricerca Interdisciplinare di Biomineralogia, Cristallografia e Biomateriali, Dipartimento di Scienze Biologiche, Geologiche e Ambientali, Università di Bologna “Alma Mater Studiorum”, Piazza di Porta San Donato 1, 40126 Bologna, Italy; riccardo.fabbri15@studio.unibo.it (R.F.); jennifer.romano@studio.unibo.it (J.R.); gianfranco.ulian2@unibo.it (G.U.); antonino.calafato@unibo.it (A.C.)
- ² Department of Civil, Chemical, Environmental and Materials Engineering, University of Bologna, 40136 Bologna, Italy; abbas.solouki2@unibo.it (A.S.); cesare.sangiorgi4@unibo.it (C.S.)
- ³ Società Azionaria Prodotti Asfaltico Bituminosi Affini (S.A.P.A.B.A. s.r.l.), 40037 Pontecchio Marconi, Italy
- * Correspondence: danielle.moro@unibo.it (D.M.); giovanni.valdre@unibo.it (G.V.)

Abstract: The present research investigates the possibility to create a silt-waste reinforced composite through a NaOH-activated, metakaolin-based geopolymerization process. In this regard, we used thermal exo–endo analysis, X-ray diffraction (XRD), and oedometric mechanical tests to characterize the produced composites. In our experimental conditions, the tested material mixtures presented exothermic peaks with maximum temperatures of about 100 °C during the studied geopolymerization process. In general, the XRD analyses showed the formation of amorphous components and new mineral phases of hydrated sodalite, natrite, thermonatrite and trona. From oedometric tests, we observed a different behavior of vertical deformation related to pressure (at RT) for the various produced composites. The present work indicated that the proposed geopolymerization process to recycle silt-waste produced composite materials with various and extended mineralogy and chemical–physical properties, largely depending on both the precursors and the specific alkaline-activating solution. Thermal analysis, XRD, and oedometric mechanical tests proved to be fundamental to characterize and understand the behavior of the newly formed composite material.

Keywords: silt waste recovery; metakaolin-based composite; geopolymerization process; thermal analysis; X-ray diffraction; mechanical and oedometric tests



Citation: Moro, D.; Fabbri, R.; Romano, J.; Ulian, G.; Calafato, A.; Solouki, A.; Sangiorgi, C.; Valdrè, G. Thermal, X-ray Diffraction and Oedometric Analyses of Silt-Waste/NaOH-Activated Metakaolin Geopolymer Composite. *J. Compos. Sci.* **2021**, *5*, 269. <https://doi.org/10.3390/jcs5100269>

Academic Editor: Francesco Tornabene

Received: 21 September 2021
Accepted: 11 October 2021
Published: 13 October 2021

Publisher's Note: MDPI stays neutral with regard to jurisdictional claims in published maps and institutional affiliations.



Copyright: © 2021 by the authors. Licensee MDPI, Basel, Switzerland. This article is an open access article distributed under the terms and conditions of the Creative Commons Attribution (CC BY) license (<https://creativecommons.org/licenses/by/4.0/>).

1. Introduction

The cement and concrete industries are responsible for approximately 7% of total CO₂ emissions into the atmosphere each year [1]. For this reason, the main objectives of the research and development of new composite materials, an alternative to those commonly used, are the recovery of waste materials (industrial and natural) and the reduction in CO₂ emissions caused by the production process [2]. For instance, Samal and coworkers studied the development of ceramics sintered using mixtures of red mud and fly ash waste materials [3]. In this context, geopolymers represent a promising type of composite material that has drawn attention for the past 30 years, because they have numerous advantages over many commonly used materials [4,5]. In fact:

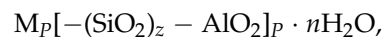
- They are produced at temperatures <100 °C, allowing significant energy savings;
- They can be produced in situ in a short time and with technologically simpler structures and equipment;
- They can use industrial waste (fly ash, ground granulated blast furnace, etc.) and low-cost natural raw materials widely spread all over the world, in particular kaolinite clays [6,7].

Due to these numerous economic and environmental advantages, geopolymers can be an important resource for the preservation of natural raw materials and the environment, for recycling waste materials and the reduction of CO₂ emissions during the production processes [8,9]. In addition, they possess adequate compressive strength, rapid hardening, thermal resistance at T > 1000 °C, resistance to acid attacks, low thermal conductivity and adhesive properties when applied to cements, steels, glass and ceramics [10–14]. Their applicative ductility allows their use in many different fields, including the construction sector, ceramics, automotive and naval industries [15]. They could be also employed for the storage of toxic/hazardous materials [15].

From the materials scientist's perspective, geopolymers are a large class of inorganic compounds based on aluminosilicate, with a polymeric structure, consisting of SiO₄ and AlO₄ tetrahedra bound together to form a three-dimensional network. The geopolymerization is a polycondensation reaction, an exothermic process that determines the formation of molecular chains made up of oligomers and other more complex structural units, linked together by covalent bonds, giving an amorphous or semi-crystalline polymeric resin similar to a cement paste [16–18]. Geopolymers are synthesized at low temperatures (below 100 °C), exploiting a chemical reaction between:

- Reactive aluminosilicate powder(s) (precursor);
- An alkaline activating solution (NaOH, KOH, sodium or potassium silicates), and;
- Appropriate fillers and/or additives.

While the above reagents are the most common ones, geopolymerization under acidic conditions exists, using phosphate-based precursors [15]. The structure of aluminosilicate geopolymers can be summarized with a generic empirical formula [17,19,20]:



where P is the degree of polycondensation, z controls the Si/Al ratio, M is a monovalent cation (Na⁺, K⁺), n is the degree of hydration of the compound. In principle, amorphous geopolymers are obtained between 20 °C and 90 °C, whereas more crystalline materials are synthesized at higher temperatures [21]. The Si/Al ratio has also an influence on the phases of neoformation obtained during the geopolymerization process, with common z values being 1, 2 or 3 [17,19,20]. With $z = 1$, the obtained geopolymers are of the poly(sialate) type, containing –Si–O–Al–O– units that form chain and ring polymers. The most common products of this family are hydrosodalite [Na₆(AlSiO₄)₆·4H₂O] and cancrinite [Na₆Ca₂(AlSiO₄)₆(CO₃)₂] [15].

Rock-forming minerals are among the most commonly employed precursors because of their wide availability. Hence, it is of paramount importance to study their mineralogical and crystal–chemical properties [15,22–24]. The most commonly used precursor is metakaolin, which is a kaolinite clay that undergoes a calcination process between 600 °C and 900 °C [25,26]. This thermal process involves the complete dehydroxylation of the starting kaolin, a reaction that is also affected by the microstrain in the mineral [27], making it highly reactive.

In the present work, a possible geopolymerization process to produce innovative composites containing waste silt has been investigated. For this purpose, we considered a low-temperature geopolymerization of poly(sialate) geopolymers, with $z = 1$, to assess its usefulness in the production of new composite materials. In addition, for practical means, we considered two commercially available metakaolin precursors and variable percentages of waste silt in the mix. The alkaline activation was a 12M sodium hydroxide solution (NaOH).

The scope of the present work is two-fold. First, we are aware that this synthetic route is extremely fast (10–20 s) at 150 °C and moderate pressures [15]. However, this could be an issue in some in situ applications, where these conditions could not be obtained. For this reason, we investigated a low-temperature and ambient pressure geopolymerization procedure to synthesize the same poly(sialate) product, which should be hydrosodalite with

the selected mixture of reagents. Secondly, there is a continuing interest in the possibility of replacing fractions of the precursors (mainly metakaolin) with a different type of waste for both recycling and sustainability purposes. As shown in a recent work [28], silt-waste from sedimentation lakes could be a possible, safe source of both precursors (e.g., kaolinite clay) and inert mineral/materials (e.g., quartz), the latter fraction acting as filler. To enhance its possible surface reactivity towards adhesion of the silt particles to the geopolymer matrix, the fine powder of the waste silt was calcinated at 850 °C.

Particular attention was paid to the characterization methods [29–35]. In the present work, the samples were thermally analyzed during the manufacturing process, namely, we measured the variation of temperature as a function of time to assess the occurrence and the heat released by the exothermic geopolymerization reaction [36]. X-Ray Diffraction analysis (XRD) was carried out on both the reagents and the geopolymer samples to characterize their mineralogy, in terms of structural variation and new phases formed during the geopolymerization process. Compression tests were finally performed to assess the mechanical stability of the composite, by measuring the vertical deformation under oedometric tests.

2. Materials and Methods

As reviewed in a very recent work [28], the recycling of the waste silt minerals was carried out by employing a geopolymerization process based on metakaolin as the starting raw material. Two commercially available metakaolins, namely Masterlife MK 828 (BASF Construction Chemicals Italia Spa, Treviso, Italy) and Metamax (BASF SE, Ludwigshafen, Germany), were used as fine powders. Masterlife MK 828 had a nominal granulometric distribution <80 µm (95%), whereas Metamax had a nominal average particle size of 1.3 µm. The average chemical analysis (weighted percentages of oxides) of the two metakaolins, as reported by the manufacturers, are shown in Table 1.

Table 1. Metakaolin and waste silt chemical composition (values reported as weighted percentages wt%).

Material	SiO ₂	Al ₂ O ₃	Na ₂ O	K ₂ O	TiO ₂	Fe ₂ O ₃	CaO	MgO	P ₂ O ₅	MnO	LOI
MK828	55	40	0.8 ^a		1.5	1.4		0.3 ^b	–	–	1.0
Metamax	52.3	45.0	0.22	0.15	1.75	0.42	0.04	0.04	0.08	–	n.r.
Waste silt _c	43.5	12.5	1.0	1.9	0.6	6.1	15.8	3.0	0.1	0.2	15.3

a—given as Na₂O + K₂O; b—given as CaO + MgO; c—uncalcinated silt [28]; LOI = loss on ignition; n.r. = data not reported.

The morphology of the metakaolin powders was investigated using a JEOL JSM-5400 Scanning Electron Microscope (SEM) equipped with a tungsten thermoionic source, working with an acceleration voltage of 20 kV. The samples were gold-coated with a layer of about 10 nm before SEM observations. Figure 1a,b show two SEM micrographs of Metamax and Masterlife MK828 powders, respectively. The morphology was dominated by booklets and platelets residual of the calcination process of the starting raw kaolin. In agreement with the granulometric data provided by the manufacturers, SEM topographical analysis revealed, on average, a lower particle size for Metamax powders (Figure 1a) than for Masterlife MK828 (Figure 1b).

Sodium hydroxide was used in form of anhydrous pellets (CAS 1310-73-2, Carlo Erba Reagents s.r.l., Cornaredo, MI, Italy) and ground with an agate mortar to prepare a 12 M solution.

As explained and detailed in the work of Solouki and coworkers [28], the waste silt was collected from S.A.P.A.B.A. s.r.l. (Bologna, Italy) sedimentation lakes, where during aggregates' production, undesirable substances such as silt, clay, and dirt are washed, separated and stored. The average chemical analysis (weighted percentages of oxides) of the uncalcinated waste silt, as provided by the cited work [28], is reported in Table 1. The waste silt was thermally treated at 850 °C for 6 h and 30 min using a static furnace before use in the geopolymerization reaction to enhance its surface reactivity [28]. This recovered

material has to be considered a filler, and it was grounded and calcinated to (i) increase its surface area, (ii) deform the particle surface and (iii) remove adsorbed and structural water. In fact, all the mineral phases found in the calcinated silt are to be considered non-reactive from the geopolymerization perspective, hence they do not alter the Si/Al ratio. The grinding and calcination treatments are intended to enhance the adhesion of the silt particles to the binder (the geopolymer matrix) [15].

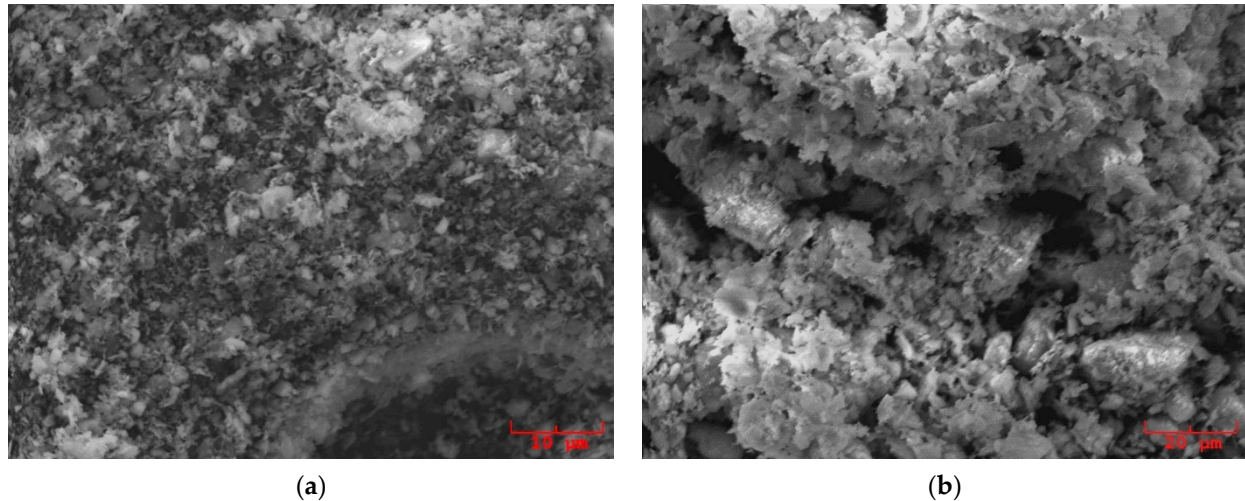


Figure 1. SEM micrographs of (a) Metamax and (b) Masterlife MK828 metakaolin powders.

The geopolymerization process was performed by mixing the metakaolin and the silt with the 12M NaOH solution for about 2 min in a cylindrical polypropylene container at room temperature ($\sim 20\text{ }^{\circ}\text{C}$), atmospheric pressure and Relative Humidity (RH) of about 40%. The container was then closed and placed in an M80-TB incubator (MPM Instruments s.r.l., Bernareggio, MB, Italy) at a curing temperature of $80\text{ }^{\circ}\text{C}$ for two hours.

In this preliminary study, six geopolymer samples were synthesized using different amounts of precursors, as summarized in Table 2. Three specimens for each mixture and test were used.

Table 2. Composition of the geopolymer sample in terms of metakaolin (Masterlife MK828 and Metamax), waste silt, and 12M NaOH solution.

Sample	MK828 [g]	Metamax [g]	Silt [g]	12M NaOH [mL]
1	10	—	—	11
2	9	—	1	11
3	7	—	3	11
4	—	10	—	11
5	—	9	1	11
6	—	7	3	11

Thermal analysis was performed during the geopolymerization process by measuring the temperature inside the polypropylene container with thermocouples and recording the temperature profiles as a function of time with a PT-104 data logger (Pico Technology Ltd., Cambridgeshire, UK). The measure of temperature versus time starts soon after the sample is placed in the incubator at $80\text{ }^{\circ}\text{C}$. For each sample, a second polypropylene container was prepared as a reference (blank), substituting the NaOH solution with bi-distilled water. Each blank was placed in the incubator simultaneously with the sample, measuring its temperature vs. time as a reference.

The mineralogical analysis was carried out by using a Philips PW 1710 X-ray diffractometer equipped with a graphite monochromator on the diffracted beam. Cu K α X-rays generated with 40 kV and 30 mA of power supply were employed. The XRD patterns

were collected from 3° to $65^\circ 2\theta$, with a step size of $0.02^\circ 2\theta$ and a counting time of 1 s/step. The specimens were prepared by using a quasi-random preparation method and the diffractograms were analyzed with the computer programs X Powder [37] and QualX2 [38].

Oedometric mechanical tests were carried out to investigate the consolidation behavior of the synthesized geopolymers. For this purpose, 1.8 g of each sample was powder grounded with an agate mortar and pre-compressed in a cylindrical cell of stainless steel (10 mm in diameter) by applying a vertical pressure of 25 MPa for 1 min and 30 s with a stainless steel piston. Each pre-compressed specimen was then subjected to two oedometric tests using vertical pressures of 30 MPa and 90 MPa for 48 h. The vertical deformation of the materials was measured using a dial gauge with a resolution of 10^{-6} m.

3. Results and Discussion

3.1. Thermal Analysis

We report in Figure 2 the thermal profiles of the six samples recorded during the geopolymerization process. Figure 2a shows the temperature variations measured for samples 1, 2, and 3, which are made with metakaolin Masterlife MK828 (see Table 1 for the specific compositions). It can be noted that each sample has an exothermic peak with a maximum temperature of 90°C for sample 1 (pure metakaolin). By including in the formulation different amounts of waste silt, the maximum recorded temperature decreased by about 3°C for sample 2 (that contains 10% of waste silt) and of 6°C for sample 3 (with 30% of waste silt). A slightly different starting time of the exothermic reaction was also observed: in fact, samples 1, 2 and 3 showed the temperature increase at 27 min, 29 min and 30 min, respectively. This exothermic reaction lasted approximately five minutes regardless of the amount of silt in the metakaolin–waste silt geopolymer composite mixture.

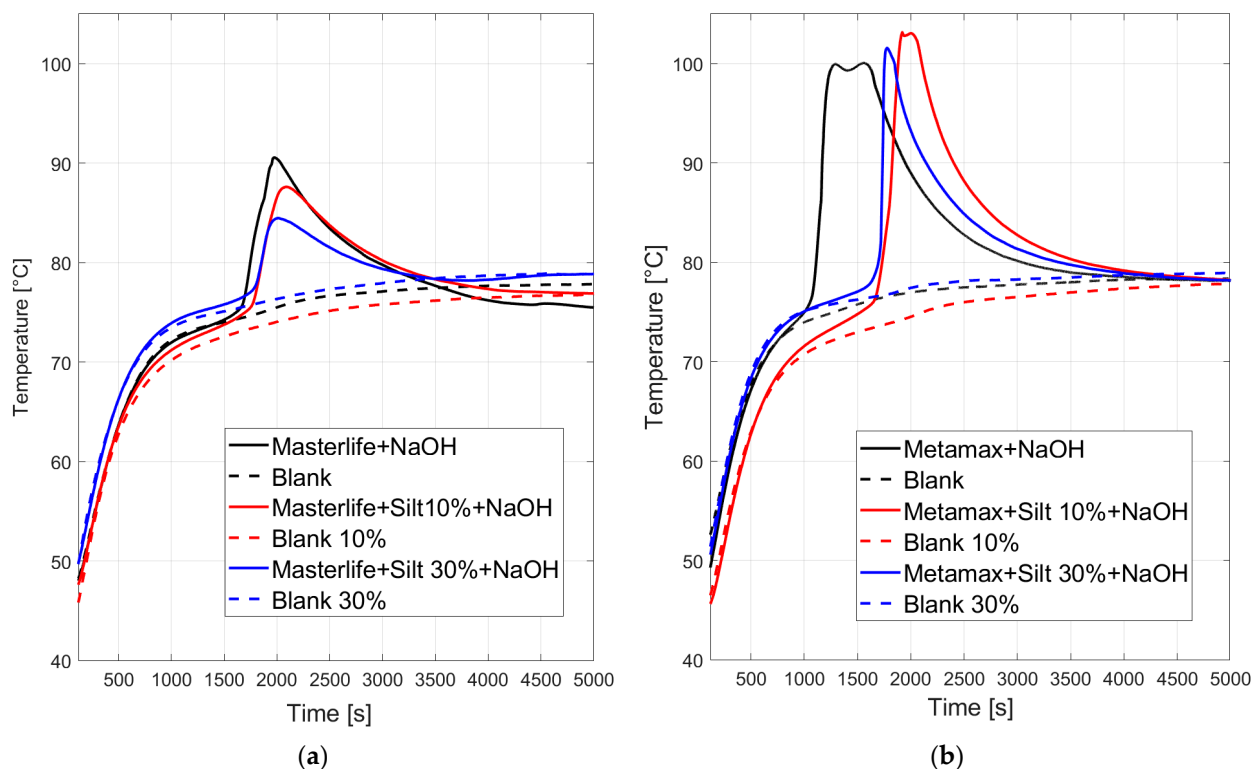


Figure 2. Thermal profiles of the geopolymer reactions: (a) samples made with metakaolin Masterlife MK828; (b) samples made with metakaolin Metamax. Black, red, and blue curves show the thermal profiles of samples 1 and 4, samples 2 and 5, samples 3 and 6, respectively.

A different behavior was observed for samples 4, 5, and 6, which were made from the Metamax metakaolin (see Figure 2b). In general, these mixtures showed a higher

maximum temperature (more than 100 °C), seemingly without any influence from the amount of the included silt. In addition, for sample 4 (pure metakaolin), a faster reaction time was observed than those recorded for Masterlife-based samples, with the exothermic reaction occurring about 10 min earlier than that of sample 1. In our experimental setup, the presence of waste silt delayed the occurrence of the exothermic peak by about 9 min compared to the pure metakaolin mixture (onset at about 18 min).

According to the thermal analysis protocol proposed by Davidovits and collaborators [36], the recorded trends suggested that metakaolin Metamax had a higher reactivity than metakaolin Masterlife MK828.

3.2. X-ray Diffraction Analysis

In the present work, XRD analyses were performed on both the precursors and the final products of the geopolymerization process to characterize the different mineralogical phases. The XRD pattern of waste silt thermally treated at 850 °C is shown with a magenta diffraction profile in Figure 3. The most intense peaks were identified as quartz, while the other peaks were associated with different silicate phases: Feldspar, a member of the solid solution gehlenite ($\text{Ca}_2\text{Al}(\text{AlSi})\text{O}_7$)—åkermanite ($\text{Ca}_2\text{MgSi}_2\text{O}_7$), diopside ($\text{CaMgSi}_2\text{O}_6$), and wollastonite (CaSiO_3). Traces of illite/mica have also been identified.

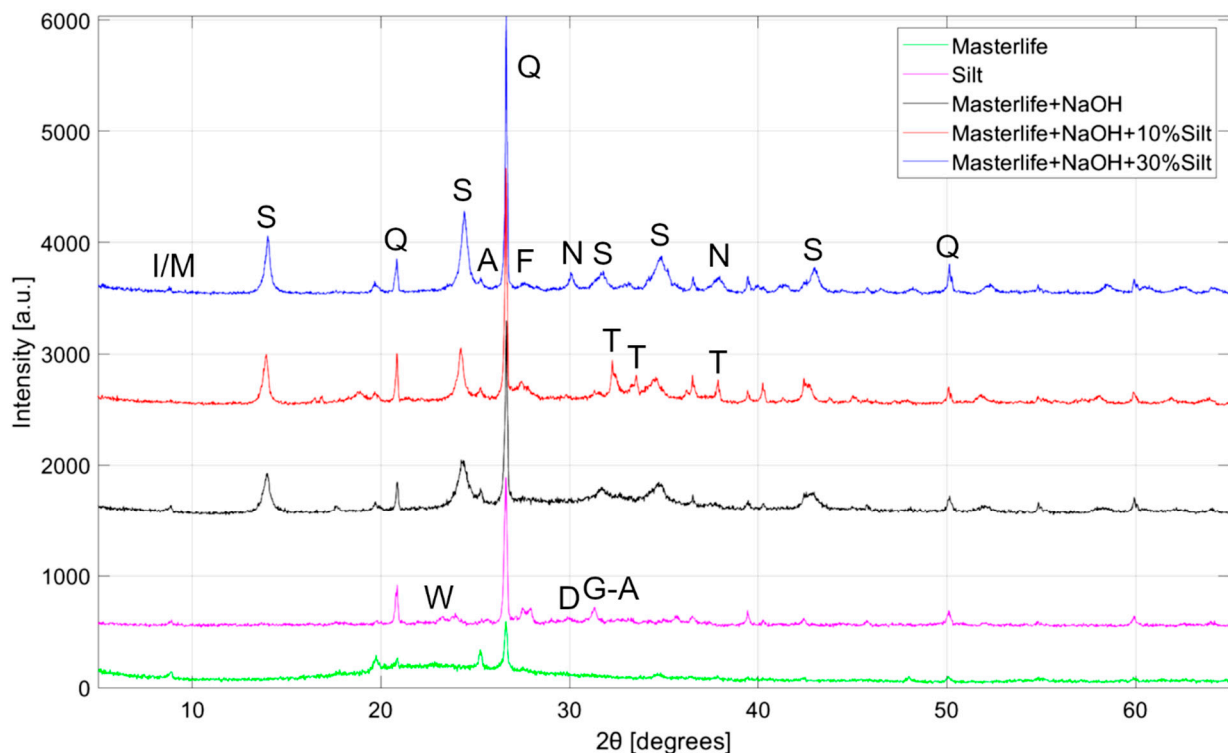


Figure 3. XRD patterns of metakaolin Masterlife MK828 (green pattern), waste silt (magenta pattern) and of samples 1, 2 and 3, made with Masterlife MK828, 12M NaOH solution and 0% (black pattern), 10% (red pattern) and 30% (blue pattern) of waste silt, respectively. The principal peaks associated with each mineralogical phase are indicated by a letter: Q = Quartz; A = Anatase; F = Feldspar; I/M = Illite/Mica; S = hydrated Sodalite; T = Thermonatrite; N = Natrite; G-A = Gehlenite—Åkermanite solid solution; D = Diopside; W = Wollastonite.

XRD patterns of the first metakaolin, Masterlife MK828, and of samples 1, 2 and 3 are also shown in Figure 3. Masterlife MK828 (green pattern) presents a typical broad amorphous hump from about 15°2θ to 35°2θ, caused by the thermal calcination process carried out by the supplier of the metakaolin. In addition, the peaks related to the mineral phases of quartz and anatase (TiO_2) have been identified. We can also see the presence of peaks related to clay mineral phases such as illite/mica, associable to residual phases of the calcination process.

The XRD pattern of sample 1 (black pattern, Figure 3), i.e., the geopolymer synthesized from the metakaolin Masterlife MK828 and the 12M NaOH solution, in comparison to that of the metakaolin precursor (green pattern), shows (i) a displacement of the hump position of about $9^\circ 2\theta$ towards higher angles, which indicates the formation of an amorphous component different from the metakaolin, and (ii) the expected hydrated sodalite $[\text{Na}_6(\text{AlSiO}_4)_6 \cdot 4\text{H}_2\text{O}]$, with well crystallized peaks. Furthermore, we can still observe residual peaks of quartz, anatase and clay minerals, which did not take part in the geopolymerization process.

The geopolymer composites of samples 2 and 3, i.e., those synthesized through the recycling of 10% (red profile) or 30% (blue profile) of silt, respectively, both present the peaks of hydrated sodalite and a reduced amorphous hump compared to that of sample 1, with comparable angular extension. Sample 2 also presents the phase of new formation thermonatrite ($\text{Na}_2\text{CO}_3 \cdot \text{H}_2\text{O}$), whereas sample 3 shows the new phase natrite (Na_2CO_3). In addition, there are residual mineral phases of anatase from metakaolin, feldspar from waste silt, and quartz and illite/mica from both metakaolin and silt.

The XRD patterns of the second metakaolin, Metamax, and samples 4, 5, and 6 are shown in Figure 4. Metamax (magenta pattern) presents a marked and typical broad amorphous hump from about $15^\circ 2\theta$ to about $35^\circ 2\theta$, caused by the efficient thermal calcination process carried out by the supplier of the metakaolin. We also noted the peaks related to anatase, the only crystalline phase in the calcinated product.

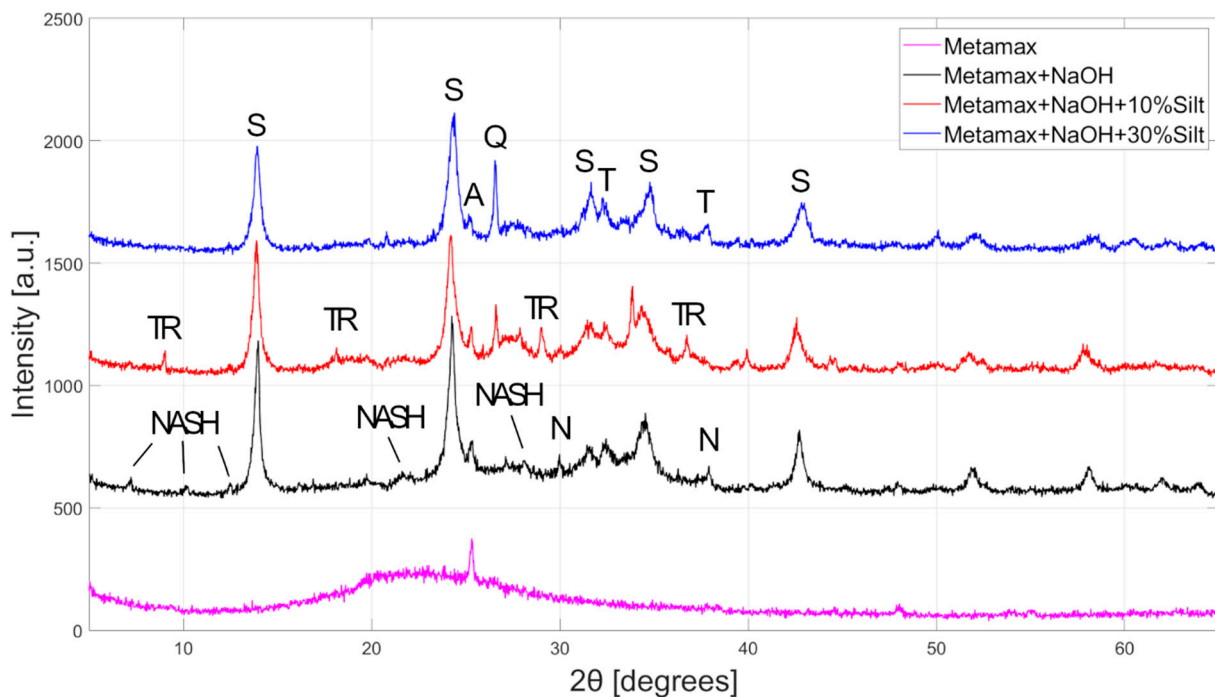


Figure 4. XRD patterns of metakaolin Metamax (magenta pattern) and of samples 4, 5 and 6, made with Metamax, 12 M NaOH solution and 0% (black pattern), 10% (red pattern), and 30% (blue pattern) of waste silt, respectively. Q = Quartz; A = Anatase; S = hydrated Sodalite; NASH = Sodium Aluminum Silicate Hydrates; T = Thermonatrite; N = Natrite; TR = Trona.

Sample 4, i.e., geopolymer synthesized from pure Metamax and 12M NaOH solution, presents an XRD pattern (black profile in Figure 4) showing an amorphous geopolymeric component with a broad hump centered about $7^\circ 2\theta$ towards higher angles, compared to that of the metakaolin precursor (magenta pattern). In addition, the peaks of neof ormation of hydrated sodalite $[\text{Na}_6(\text{AlSiO}_4)_6 \cdot 4\text{H}_2\text{O}]$, and minor presence of other sodium aluminum silicate hydrates (NASH), thermonatrite ($\text{Na}_2\text{CO}_3 \cdot \text{H}_2\text{O}$) and natrite (Na_2CO_3) were revealed, together with traces of residual anatase. Among the newly formed crystalline phases, hydrated sodalite was the most abundant.

The XRD patterns of samples 5 and 6, synthesized with 10% (red pattern) and 30% (blue pattern) of waste silt in the solid mixture, respectively, present the hump of amorphous geopolymer component from about $15^{\circ}2\theta$ to about $40^{\circ}2\theta$, similarly to that observed for sample 4. Hydrated sodalite and minor presence of sodium aluminum silicate hydrates and thermonatrite were phases of new formation. Sample 5 also presents the new phase trona [$\text{Na}_3(\text{HCO}_3)(\text{CO}_3)\cdot 2\text{H}_2\text{O}$] and traces of natrite. As already observed for samples synthesized with Masterlife MK828, hydrated sodalite was the most abundant crystalline phase of neoformation. Finally, anatase and quartz, which are residuals of the calcination process of metakaolin and the waste silt, respectively, were found in the final product.

In general, the mineralogical composition of the synthesized geopolymers is complex, with the presence of large amounts of the amorphous phase. In all synthesized samples, an amorphous phase and hydrated sodalite (expected crystalline phase) are the most abundant products of the reaction. They are almost the only phases of neoformation when no waste silt is present in the reagents. The new (and residual) phases in the geopolymerization product are the same ones reported by J. Davidovits [39], but it is worth noting that we did not apply any pressure to the mixture and the synthetic route was performed at a much lower temperature than 150°C . According to previous studies of J. Davidovits [15,21], the presence of only an amorphous phase and hydrated sodalite suggests that all precursors reacted with the activating solution of sodium hydroxide to form only aluminosilicate materials.

By partially replacing the metakaolin with waste silt, the formation of other mineral phases can be noted. In particular hydrated and anhydrous sodium carbonates (natrite, thermonatrite, trona), which are accessory with respect to both the geopolymeric matrix and hydrated sodalite. It is a known issue for alkali-activated binders, which may be subject to carbonation processes when exposed to carbon dioxide-rich environments [40]. For example, in the study of Bernal and coworkers [41] it was shown the formation of trona in a geopolymer sample synthesized with granular blast furnace slag, whereas Puertas et al. [40,42] observed the formation of natron ($\text{Na}_2\text{CO}_3\cdot 10\text{H}_2\text{O}$) in alkali-activated slag mortars.

In the present work, we did not perform any carbonation procedure during sample preparation; hence, it was expected that CO_2 was absorbed from the atmosphere. This can be justified by the low concentration of sodium (bi)carbonates in our products when compared to the previously cited studies [40–42]. In addition, it is in accordance with the study conducted by De Vargas and coworkers [43], who characterized by XRD geopolymeric binders made of mixtures of fly ash and metakaolin cured at room temperature and pressure, finding natrite in the geopolymeric products. The mineralogy of the sodium carbonate phases in samples 1–6 can be explained by the different alkalinity of the pore solution, i.e., the alkaline solution present in the pores of the hardened geopolymeric material, which may be influenced by any residual NaOH activating solution, as proposed by Bernal and colleagues [41]. Sample 1 contains no carbonated phase, thus, it can be supposed that all the sodium hydroxide solution quantitatively reacted with the Masterlife MK828 metakaolin, hence, all Na^+ ions were included in the geopolymeric (amorphous) or hydrated sodalite phases. When the metakaolin was partially replaced with waste silt, the presence of thermonatrite (sample 2) and natrite (sample 3) suggested that more sodium ions were available in the pore solutions for crystallization. In fact, as also studied by Solouki et al. [28] for the synthesis of geopolymers with Si:Al = 2:1 ratio, the silt was not reactive towards geopolymerization and acted only as a filler.

Sample 4 shows an interesting composition, because, although it was made from pure Metamax metakaolin, it presented a very small amount of natrite. This means that a very small amount of Na^+ from the activating 12 M NaOH solution was still available in the pore solution. In addition, the presence of NASH material other than hydrated sodalite suggests that this phase could have been formed because of the high reactivity of Metamax (see Figure 2b), which may be associated with a low selectivity of the products. Sample 5 was synthesized with 10% of waste silt and contains trona as a product, a sodium bicarbonate

phase, whereas thermonatrite was obtained in sample 6 (30% of waste silt). The presence of the sodium carbonate phases is in agreement with the previous discussion on samples 2 and 3. However, since the pKa of the $\text{CO}_3^{2-}/\text{HCO}_3^-$ equilibrium is around 10.3, trona is only expected to form when the pore solution pH is equal to that value, whereas at higher pH values thermonatrite and natrite are formed. These considerations are in line with previous observations found in the literature [40–42].

As expected, quartz and anatase do not participate in the geopolymeric process, because they are stable in the reaction conditions of high pH and low temperature.

3.3. Oedometric Mechanical Tests

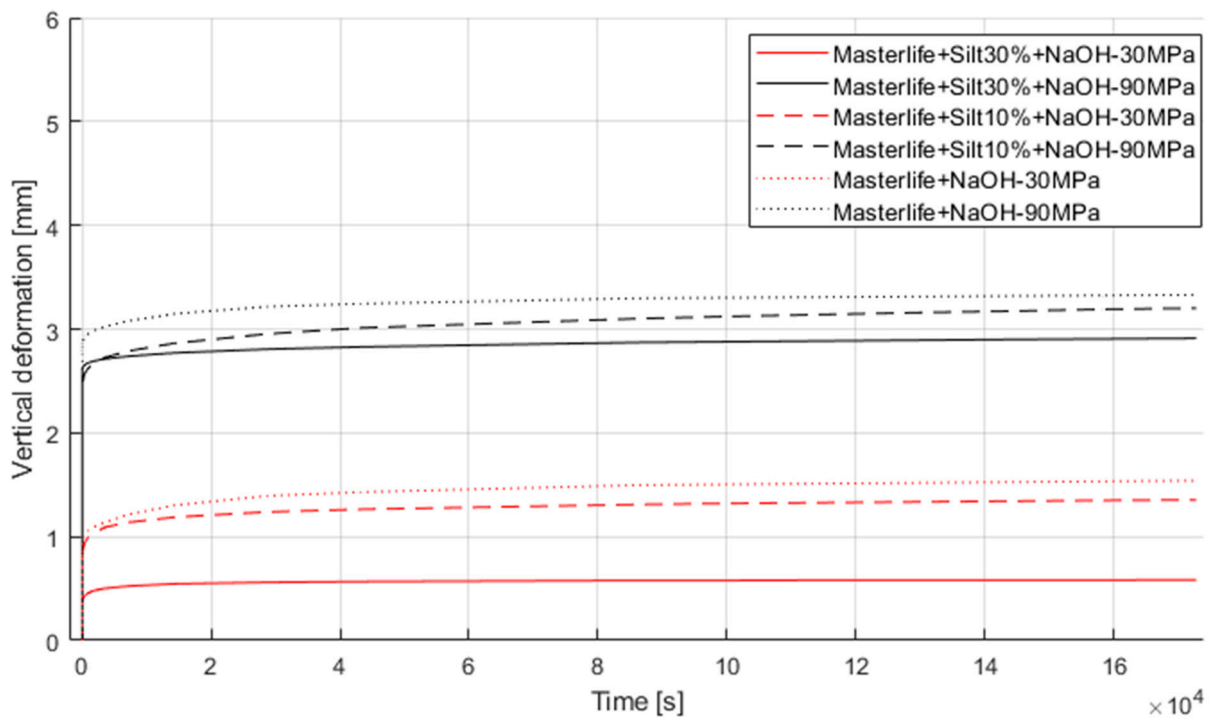
Oedometric mechanical tests were performed to evaluate the consolidation behavior of composite geopolymeric powders synthesized with (samples 2, 3, 5 and 6) and without (samples 1 and 4) the recovery of waste silt. The consolidation behavior of each sample was investigated for 48 h using a vertical pressure of 30 MPa and 90 MPa. The results are graphically reported in Figure 5, where the vertical deformation of the different samples as a function of time is shown.

In our experimental setup, the geopolymer made of Masterlife MK828 (sample 1, Figure 5a) showed a vertical deformation, at 48 h, of about 1.54 mm at 30 MPa and about 3.33 mm at 90 MPa. The composite geopolymer formulation with 10% of silt (sample 2) had a vertical deformation of about 1.35 mm and 3.20 mm at 30 MPa and 90 MPa, respectively. By increasing the silt fraction to 30% (sample 3), a reduction of the vertical deformation could be noted, with maximum values of 0.58 mm (30 MPa) and 2.91 mm (90 MPa).

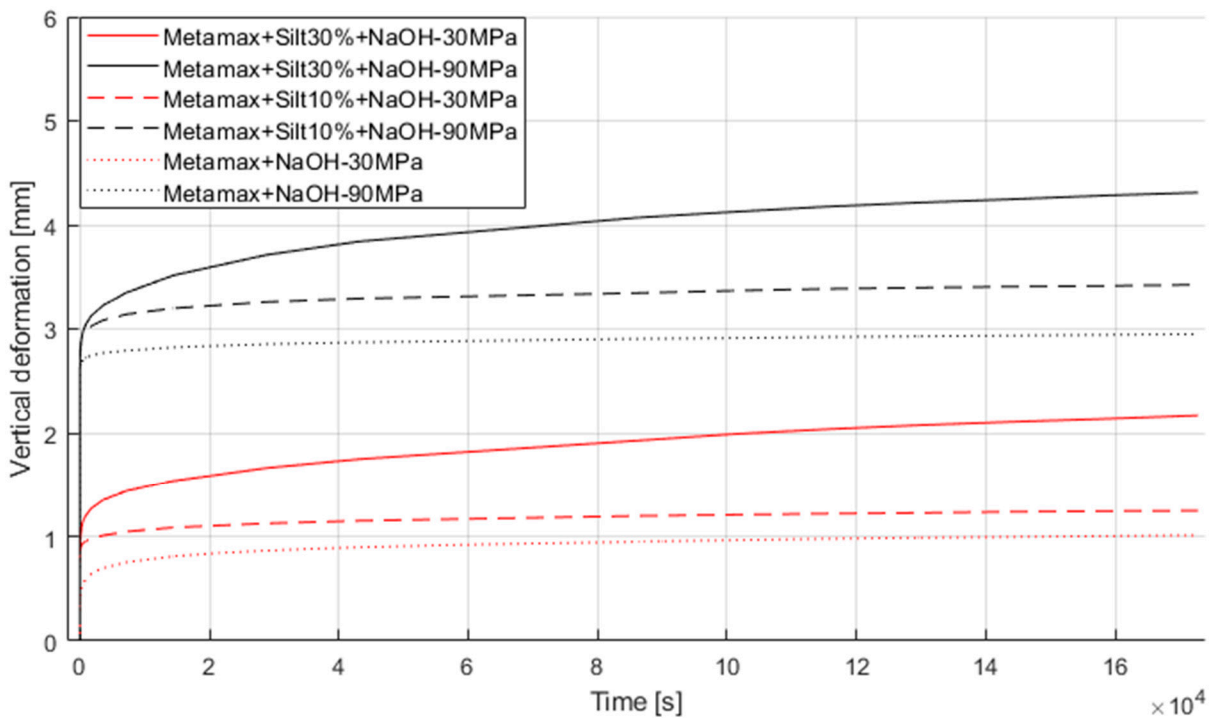
The composite geopolymers made with Metamax metakaolin (samples 4, 5 and 6, Figure 5b) show a different behavior depending on the silt fraction. In fact, the pure metakaolin geopolymer (sample 4), after 48 h, was vertically deformed at 30 MPa by about 1.01 mm and at 90 MPa by about 2.95 mm. With respect to sample 1 (Masterlife MK828) the geopolymer made with Metamax showed a lower deformation. However, differently from Masterlife MK828 geopolymer composites, the increase in silt resulted in an increased vertical deformation. In fact, sample 5 (made with 10% of waste silt) has a vertical deformation of about 1.25 mm and 3.42 mm at 30 MPa and 90 MPa, respectively. For sample 6 (made with 30% of waste silt) the recorded vertical deformation at 48 h was 2.16 mm (30 MPa) and 4.31 mm (90 MPa).

In the last 4 h (time of last acquisition) Masterlife-based geopolymers had a vertical deformation, at 30 MPa and 90 MPa, of about 7 μm and 6 μm (sample 1), 4 μm and 11 μm (sample 2), and 3 μm and 5 μm (sample 3), respectively. Conversely, Metamax-based geopolymers had a vertical deformation, at 30 MPa and 90 MPa, of about 8 μm and 7 μm (sample 4), 4 μm and 11 μm (sample 5), and 33 μm and 28 μm (sample 6).

As expected, the observed behaviors depend on various factors, including the different mineralogy, the physical characteristics of the samples, such as the porosity, and the type of metakaolin used as a precursor. As previously described, the amount of silt in the mixture affects the ratio between the main products (amorphous geopolymer and hydrosodalite) and carbonated phases (natrite, thermonatrite and trona). The geopolymerization product is then a composite material, whose macroscopic mechanical properties are controlled by those of each component, by the particle size and distribution within the material and the interfaces between each particle. For example, the higher compressibility of sample 2 compared to sample 3 can be explained by the presence of thermonatrite ($\text{Na}_2\text{CO}_3 \cdot \text{H}_2\text{O}$) in the former and natrite (anhydrous Na_2CO_3) in the latter. In fact, the structural water of thermonatrite could be one of the reasons for the softer behavior of sample 2. The same consideration could be extended to samples 5 and 6, but in this case, it seems that trona confers less compressibility to the composite product, although presenting more structural water molecules than thermonatrite. In this sense, more information on the elasticity of the different sodium (bi)carbonate phases is required to fully address the present results.



(a)



(b)

Figure 5. Oedometric tests on samples using vertical pressures of 30 MPa and 90 MPa (red and black curves, respectively) for 48 h: panel (a) shows sample 1 (dotted line), sample 2 (continuous line) and 3 (dashed line), panel (b) shows sample 4 (dotted line), sample 5 (continuous line) and 6 (dashed line).

4. Conclusions

In the present study, composite geopolymers containing different percentages of waste silt made with two commercial metakaolins and Si:Al = 1 were investigated and characterized in detail from a thermal, mineralogical and mechanical point of view. The

advantage of the considered Si:Al ratio is that it is already provided by the sole metakaolin precursor and no reagent other than the alkali activating solution is required. In fact, to obtain geopolymers with Si:Al > 1 it is necessary to add sodium metasilicate, sodium disilicate, or other reactive materials containing silica. The waste silt used in the present work has to be considered as a filler. In this regard, further studies are needed to optimize the adhesion of the waste silt particles with the geopolymeric binder.

From the thermal point of view, the characterization of the reactivity of the metakaolin precursors is important for the development of geopolymer formulations and operative procedures of the binder with and without the presence of any filler. In this context, Metamax showed a higher reactivity than Masterlife MK828, which in both cases was affected by the presence of waste silt.

The mineralogical characterization allowed us to identify an amorphous component and hydrated sodalite as the main phases of neoformation in all the investigated samples. Natrite, thermonatrite and trona, which are sodium (bi)carbonate phases, seem to be associated with the presence of Na⁺ ions and different alkalinity of pore solution. Some residual mineral phases, remaining from the metakaolin precursors and the waste silt, and not participating in the geopolymer reaction, such as quartz and anatase, were also identified.

An inverse trend of the vertical deformation was observed for Masterlife-based and Metamax-based samples, the first presenting lower vertical deformations while increasing the silt fraction from 10% to 30%, the second showing an opposite trend. Such behavior seems mainly governed by the different mineralogy of the composite samples.

This initial study indicates and confirms that it is possible to recycle waste silt to create well consolidated new composite materials, such as geopolymers, and their mechanical resistance was investigated by preliminary oedometric tests. Future studies are envisaged to try to enhance the quality of the formula of mixtures and increase mechanical properties of these composite and innovative materials and/or increase the percentage of waste silt recovery and recycling while maintaining the sufficient performance of the final products.

Author Contributions: Conceptualization, D.M., C.S., A.S., G.U. and G.V.; methodology, A.C., D.M., R.F., J.R. and G.V.; validation, D.M., G.U., A.S., C.S. and G.V.; formal analysis, D.M., A.C., R.F., J.R., G.U., A.S., C.S. and G.V.; investigation, D.M., A.C., R.F., J.R., G.U. and G.V.; data curation, D.M., A.C., R.F., J.R., G.U. and G.V.; Writing—Original draft preparation, D.M., R.F., J.R., G.U. and G.V.; Writing—Review and editing, D.M., R.F., J.R., G.U., A.S., C.S. and G.V.; supervision, C.S. and G.V. All authors have read and agreed to the published version of the manuscript.

Funding: Part of the presented research was conducted as part of the SAFERUP! Project, which has received funding from the European Union's Horizon 2020 research and innovation program under the Marie Skłodowska-Curie grant agreement No 765057.

Conflicts of Interest: The authors declare no conflict of interest.

References

1. Sanjuán, M.Á.; Andrade, C.; Mora, P.; Zaragoza, A. Carbon Dioxide Uptake by Cement-Based Materials: A Spanish Case Study. *Appl. Sci.* **2020**, *10*, 339. [[CrossRef](#)]
2. Sood, D.; Hossain, K.M.A. Optimizing Precursors and Reagents for the Development of Alkali-Activated Binders in Ambient Curing Conditions. *J. Compos. Sci.* **2021**, *5*, 59. [[CrossRef](#)]
3. Samal, S.; Ray, A.K.; Bandopadhyay, A. Characterization and microstructure observation of sintered red mud–fly ash mixtures at various elevated temperature. *J. Clean. Prod.* **2015**, *101*, 368–376. [[CrossRef](#)]
4. Solouki, A.; Viscomi, G.; Lamperti, R.; Tataranni, P. Quarry Waste as Precursors in Geopolymers for Civil Engineering Applications: A Decade in Review. *Materials* **2020**, *13*, 3146. [[CrossRef](#)] [[PubMed](#)]
5. Zakka, W.P.; Abdul Shukor Lim, N.H.; Chau Khun, M. A scientometric review of geopolymer concrete. *J. Clean. Prod.* **2021**, *280*, 124353. [[CrossRef](#)]
6. Duxson, P.; Fernández-Jiménez, A.; Provis, J.L.; Lukey, G.C.; Palomo, A.; van Deventer, J.S.J. Geopolymer technology: The current state of the art. *J. Mater. Sci.* **2007**, *42*, 2917–2933. [[CrossRef](#)]
7. Panagiotopoulou, C.; Kontori, E.; Perraki, T.; Kakali, G. Dissolution of aluminosilicate minerals and by-products in alkaline media. *J. Mater. Sci.* **2006**, *42*, 2967–2973. [[CrossRef](#)]
8. Van Deventer, J.S.J.; Provis, J.L.; Duxson, P.; Brice, D.G. Chemical Research and Climate Change as Drivers in the Commercial Adoption of Alkali Activated Materials. *Waste Biomass Valorization* **2010**, *1*, 145–155. [[CrossRef](#)]

9. Taki, K.; Mukherjee, S.; Patel, A.K.; Kumar, M. Reappraisal review on geopolymer: A new era of aluminosilicate binder for metal immobilization. *Environ. Nanotechnol. Monit. Manag.* **2020**, *14*, 100345. [CrossRef]
10. Davidovits, J. Geopolymers: Ceramic-like inorganic polymers. *J. Ceram. Sci. Technol.* **2017**, *8*, 335–350. [CrossRef]
11. Provis, J.L.; Van Deventer, J.S.J. (Eds.) *Geopolymers. Structures, Processing, Properties and Industrial Applications*, 1st ed.; Woodhead Publishing: Cambridge, UK, 2009; ISBN 978-1-84569-449-4.
12. Provis, J.L. Alkali-activated materials. *Cem. Concr. Res.* **2018**, *114*, 40–48. [CrossRef]
13. Pacheco-Torgal, F.; Castro-Gomes, J.; Jalali, S. Alkali-activated binders: A review: Part 1. Historical background, terminology, reaction mechanisms and hydration products. *Constr. Build. Mater.* **2008**, *22*, 1305–1314. [CrossRef]
14. Pacheco-Torgal, F.; Castro-Gomes, J.; Jalali, S. Alkali-activated binders: A review. Part 2. About materials and binders manufacture. *Constr. Build. Mater.* **2008**, *22*, 1315–1322. [CrossRef]
15. Davidovits, J. *Geopolymer Chemistry and Applications*, 5th ed.; Davidovits, J., Ed.; Institut Géopolymère: Saint-Quentin, France, 2020; ISBN 9782954453118.
16. Xu, H.; Van Deventer, J.S.J. Geopolymerisation of multiple minerals. *Miner. Eng.* **2002**, *15*, 1131–1139. [CrossRef]
17. Khale, D.; Chaudhary, R. Mechanism of geopolymerization and factors influencing its development: A review. *J. Mater. Sci.* **2007**, *42*, 729–746. [CrossRef]
18. Phair, J.W.; Van Deventer, J.S.J. Effect of silicate activator pH on the leaching and material characteristics of waste-based inorganic polymers. *Miner. Eng.* **2001**, *14*, 289–304. [CrossRef]
19. Komnitsas, K.; Zaharaki, D. Geopolymerisation: A review and prospects for the minerals industry. *Miner. Eng.* **2007**, *20*, 1261–1277. [CrossRef]
20. Pacheco-Torgal, F.; Abdollahnejad, Z.; Miraldo, S.; Baklouti, S.; Ding, Y. An overview on the potential of geopolymers for concrete infrastructure rehabilitation. *Constr. Build. Mater.* **2012**, *36*, 1053–1058. [CrossRef]
21. Davidovits, J. Geopolymers. *J. Therm. Anal.* **1991**, *37*, 1633–1656. [CrossRef]
22. Ulian, G.; Valdrè, G. Density functional investigation of the thermophysical and thermochemical properties of talc $[Mg_3Si_4O_{10}(OH)_2]$. *Phys. Chem. Miner.* **2015**, *42*, 151–162. [CrossRef]
23. Ulian, G.; Valdrè, G.; Corno, M.; Ugliengo, P. DFT investigation of structural and vibrational properties of type B and mixed A-B carbonated hydroxylapatite. *Am. Mineral.* **2014**, *99*, 117–127. [CrossRef]
24. Gatta, G.D.; Merlini, M.; Valdrè, G.; Liermann, H.-P.; Nénert, G.; Rothkirch, A.; Kahlenberg, V.; Pavese, A. On the crystal structure and compressional behavior of talc: A mineral of interest in petrology and material science. *Phys. Chem. Miner.* **2013**, *40*, 145–156. [CrossRef]
25. Ferone, C.; Liguori, B.; Capasso, I.; Colangelo, F.; Cioffi, R.; Cappelletto, E.; Di Maggio, R. Thermally treated clay sediments as geopolymer source material. *Appl. Clay Sci.* **2015**, *107*, 195–204. [CrossRef]
26. Zhang, F.; Zhang, L.; Liu, M.; Mu, C.; Liang, Y.N.; Hu, X. Role of alkali cation in compressive strength of metakaolin based geopolymers. *Ceram. Int.* **2017**, *43*, 3811–3817. [CrossRef]
27. Dellisanti, F.; Valdrè, G. The role of microstrain on the thermostructural behaviour of industrial kaolin deformed by ball milling at low mechanical load. *Int. J. Miner. Process.* **2012**, *102–103*, 69–77. [CrossRef]
28. Solouki, A.; Fathollahi, A.; Viscomi, G.; Tataranni, P.; Valdrè, G.; Coupe, S.J.; Sangiorgi, C. Thermally Treated Waste Silt as Filler in Geopolymer Cement. *Materials* **2021**, *14*, 5102. [CrossRef]
29. Sambucci, M.; Sibai, A.; Valente, M. Recent Advances in Geopolymer Technology. A Potential Eco-Friendly Solution in the Construction Materials Industry: A Review. *J. Compos. Sci.* **2021**, *5*, 109. [CrossRef]
30. Hanzlíček, T.; Perná, I.; Uličná, K.; Římal, V.; Štěpánková, H. The Evaluation of Clay Suitability for Geopolymer Technology. *Minerals* **2020**, *10*, 852. [CrossRef]
31. Duxson, P.; Provis, J.L.; Lukey, G.C.; Mallicoat, S.W.; Kriven, W.M.; Van Deventer, J.S.J. Understanding the relationship between geopolymer composition, microstructure and mechanical properties. *Colloids Surf. A Physicochem. Eng. Asp.* **2005**, *269*, 47–58. [CrossRef]
32. Moro, D.; Ulian, G.; Valdrè, G. Nanoscale cross-correlated AFM, Kelvin probe, elastic modulus and quantum mechanics investigation of clay mineral surfaces: The case of chlorite. *Appl. Clay Sci.* **2016**, *131*, 175–181. [CrossRef]
33. Gatti, A.; Valdre, G.; Tombesi, A. Importance of microanalysis in understanding mechanism of transformation in active glassy biomaterials. *J. Biomed. Mater. Res.* **1996**, *31*, 475–480. [CrossRef]
34. Valdrè, G.; Botton, G.A.; Brown, L.M. High spatial resolution PEELS characterization of FeAl nanograins prepared by mechanical alloying. *Acta Mater.* **1999**, *47*, 2303–2311. [CrossRef]
35. Borgia, G.C.; Brown, R.J.S.; Fantazzini, P.; Mesini, E.; Valdre, G. Diffusion-weighted spatial information from 1H relaxation in restricted geometries. *Nuovo Cim. D* **1992**, *14*, 745–759. [CrossRef]
36. Davidovits, R.; Plelegris, C.; Davidovits, J. *Standardized Method in Testing Commercial Metakaolins for Geopolymer Formulations*; Institut Géopolymère: Saint-Quentin, France, 2019.
37. Martín-Ramos, J.D. *Using X Powder: A Software Package for Powder X-ray Diffraction Analysis*; 2004; ISBN 84-609-1497-6. User Guide; Available online: <http://www.xpowder.com/download/xpowder.pdf> (accessed on 12 October 2021).
38. Altomare, A.; Corriero, N.; Cuocci, C.; Falcicchio, A.; Moliterni, A.; Rizzi, R. QUALX2.0: A qualitative phase analysis software using the freely available database POW_COD. *J. Appl. Crystallogr.* **2015**, *48*, 598–603. [CrossRef]

39. Davidovits, J. Process for Agglomerating Compressible Mineral Substances in the Form of Powder Particles or Fibres. U.S. Patent GB1481479A, 7 June 1977.
40. Puertas, F.; Palacios, M.; Vázquez, T. Carbonation process of alkali-activated slag mortars. *J. Mater. Sci.* **2006**, *41*, 3071–3082. [[CrossRef](#)]
41. Bernal, S.A.; de Gutierrez, R.M.; Provis, J.L.; Rose, V. Effect of silicate modulus and metakaolin incorporation on the carbonation of alkali silicate-activated slags. *Cem. Concr. Res.* **2010**, *40*, 898–907. [[CrossRef](#)]
42. Palacios, M.; Puertas, F. Effect of Carbonation on Alkali-Activated Slag Paste. *J. Am. Ceram. Soc.* **2006**, *89*, 3211–3221. [[CrossRef](#)]
43. De Vargas, A.S.; De Gutierrez, R.M.; Castro-Gomes, J. *Study of Geopolymeric Binders of Fly Ash/Metakaolin Mixtures Cured at Room Temperature*; Trans Tech Publications: Bäch SZ, Switzerland, 2014; Volume 600, ISBN 9783037859810.